Peak Estimation of Univariate Spectra by the Best $L1$ Piecewise Monotonic Approximation Method

IOANNIS C. DEMETRIOU and IOANNIS N. PERDIKAS
National and Kapodistrian University of Athens
Department of Economics, Division of Mathematics and Informatics
1 Sofokleous and Aristidou Street, 105 59 Athens
GREECE

Abstract: We consider applications of the best L_1 piecewise monotonic approximation method for the peak estimation of three sets of up to 2500 measurements of Raman, Infrared and Nuclear Magnetic Resonance (NMR) spectra. Peak estimation is an inherent problem of spectroscopy. The location of peaks and their intensities are the signature of a sample of an organic or an inorganic compound. The diversity and the complexity of our measurements makes it a difficult test of the effectiveness of the method. We find that the method identifies efficiently peaks and we compare to the results obtained by the analogous least squares calculations. These results have many similarities and occasionally considerable differences due to both properties of the norms employed in the optimization calculations and nature of the spectra. Our results may be helpful to subject analysts as part of the information on which decisions will be made for estimating peaks in sequences of spectra and to the development ofnewalgorithmsthatareparticularlysuitableforpeakestimationcalculations.

Key–Words: data approximation, diiodothyronine, first differences, infrared, least squares, L_1-norm, nuclear magneticresonance,peakestimation,piecewisemonotonic,Raman,spectroscopy,sulfoniumdeuterated,zircon

Received: Febuary 28, 2020. Revised: August 16, 2020. Accepted: September 13, 2020. Published: October 2, 2020.

1 Introduction

Recently, Demetriou and Perdikas [11] have presented examples of peak estimation to measurements of Raman, Infrared and NMR spectra by the piecewise monotonic data approximation method where the smoothing criterion is the L_2 norm (least squares). In this work we investigate the performance of the piecewise monotonic approximation method with respect to the L_1 norm on the same data sets and we demonstrate that these norms lead occasionally to different results in peak estimation. The given calculations may help the analyst to comprehend strengths and differences of both these methods in their spectral analyses.

Peak estimation is a problem of continuous interest in spectroscopy and chromatography and many similar problems appear, for instance in biology, analytical chemistry, data science, energy, finance, physics and time series calculations. Peak estimation problems appear inherently in spectroscopy. In general, each peak in a spectrum corresponds to an element which is unique in terms of strength and location for the sample type (see, for example, [17], [20] and [26]).

The problem of the piecewise monotonic data approximation method with respect to the least squares norm was studied in depth by Demetriou and Powell [12] and is defined as follows. Let $\{\phi_i : \ i = 1, 2, \ldots, n\}$ be a sequence of values of a function $f(x)$ measured at the abscissae $\{x_i : \ i = 1, 2, \ldots, n\}$, where the abscissae increase strictly monotonically, but the measurements include errors, and the data are to be used to estimate the turning points of the function. We assume that if the function has turning points, then the number of measurements is substantially greater than the number of turning points. Therefore we modify the measurements if their first differences $\{\phi_{i+1} - \phi_i : \ i = 1, \ldots, n-1\}$ include more than $k-1$ sign changes, where k is a prescribed integer. This condition allows k monotonic sections to the smoothed values $\{y_i : \ i = 1, 2, \ldots, n\}$. We regard the original data and the smoothed values as n-vectors, $\boldsymbol{\phi}$ and $\boldsymbol{y}$ say.

In this paper, we give particular attention to the use of the L_1 norm. Specifically, the numbers $\{y_i : i = 1, 2, \ldots, n\}$ are calculated by minimizing the sum of the moduli of residuals

$$\Phi(\boldsymbol{y}) = \sum_{i=1}^{n} |y_i - \phi_i| \quad (1)$$

subject to the piecewise monotonicity constraints

$$\left.\begin{array}{l} y_{t_{j-1}} \leq y_{t_{j-1}+1} \leq \cdots \leq y_{t_j}, \ j \text{ is odd} \\ y_{t_{j-1}} \geq y_{t_{j-1}+1} \geq \cdots \geq y_{t_j}, \ j \text{ is even} \end{array}\right\}, \quad (2)$$

where the integers $\{t_j : \ j = 1, 2, \ldots, k-1\}$ satisfy the conditions

$$1 = t_0 \leq t_1 \leq \cdots \leq t_k = n. \quad (3)$$

We call $\boldsymbol{y}$ a best L_1 piecewise monotonic approximation to $\boldsymbol{\phi}$, and we call peak the value y_{t_j}, for even j in $[1, k-1]$.

It is important to note that the integers $\{t_j : \ j = 1, 2, \ldots, k-1\}$ are not known in advance, but their values are to be found automatically by the optimization calculation, which is a combinatorial problem.

An efficient method for this calculation and a Fortran software package that implements the method have been developed by Demetriou [6], [7] respectively. The software is named L1PMA. In general, a best approximation in the sense of the L_1 norm has the remarkable property, which makes it particularly suitable to data smoothing when there are few gross errors in the data, that the magnitudes of the errors make no difference to the best fit (see, for example, Powell [24]).

Two advantages of the piecewise monotonicity approximation technique over other smoothing techniques problem are as follows. First, there is no need to choose a set of approximating functions as for example in splines or wavelets (see, for example, de Boor [3], and Holschneider [18]). Second, the smoothing process is a projection because, if it is applied to the smoothed values, then no changes are made to.

This paper is concerned with applications of the best L_1 piecewise monotonic data approximation method to peak estimation of univariate spectra. Specifically, it extends the numerical examples of Demetriou and Perdikas [11] that minimize the objective function $\sum_{i=1}^{n}(y_i - \phi_i)^2$ subject to the same constraints to the L_1 case.

The paper is organized as follows. A brief description of the best L_1 piecewise monotonic data approximation is given in Section 2. Then three examples that illustrate the estimations of peaks in Raman, Infrared and NMR samples are presented in Section 3. The numerical results are analyzed, the effectiveness of the method for peak estimation is demonstrated and, a direct comparison is made between these results and those obtained by the analogous least squares method. Some concluding remarks and discussion on the possibility of future directions of this research are presented in Section 4.

The calculations were performed on a HP 8770w portable workstation with an Intel Core i7-3610QM, 2.3 GHz processor, which was used with the standard Fortran compiler of the Intel Visual Fortran Composer XE2013 in single precision arithmetic operating on Windows 7 with 64 bits word length.

2 Best L_1 Piecewise Monotonic Data Approximation

This section describes briefly the best L_1 piecewise monotonic approximation problem. As was already noted, the main difficulty in a piecewise monotonic calculation is that the integers $\{t_j : \ j = 1, 2, \ldots, k-1\}$ are also variables of the optimization problem. There are $\mathcal{O}(n^{k-1})$ combinations of these integers in order to find a combination that gives an optimal approximation. Therefore, it would not be practicable to test each combination separately. In addition, any general optimization algorithm will stop at a local minimum that need not be a global one.

However, much less work is needed, because of a decomposition property of the L_1 optimal solution (see, Demetriou [10]), which depends on the following two properties of the solution. If $\boldsymbol{y}$ is optimal, then optimality admits the interpolation conditions

$$y_{t_j} = \phi_{t_j}, j = 1, 2, \ldots, k-1, \quad (4)$$

and the optimal components $\{y_i : i = t_{j-1}, t_{j-1} + 1, \ldots, t_j\}$, $1 \leq j \leq k$ of the jth monotonic section of $\boldsymbol{y}$ have the values that minimize the sum of moduli

$$\sum_{i=t_{j-1}}^{t_j} |y_i - \phi_i| \quad (5)$$

subject only to the constraints

$$y_i \leq y_{i+1}, i = t_{j-1}, \ldots, t_j - 1, \ \text{ if } j \text{ is odd} \quad (6)$$

or subject to the constraints

$$y_i \geq y_{i+1}, i = t_{j-1}, \ldots, t_j - 1, \ \text{ if } j \text{ is even.} \quad (7)$$

Therefore, provided that $\{t_i : \ i = 1, 2, \ldots, k-1\}$ are known, the components of $\boldsymbol{y}$ can be generated by solving a separate monotonic problem on each section

$[t_{j-1}, t_j]$. Further, we let $\alpha(t_{j-1}, t_j)$ be the least value of (5) subject to the constraints (6), $\beta(t_{j-1}, t_j)$ be the least value of (5) subject to the constraints (7), and $\gamma(k, n)$ be the value of the objective function $\Phi(\boldsymbol{y})$ at an optimal vector. Hence, in view of these properties, we express $\gamma(k, n)$ in the form

$$\gamma(k,n) = \\ \alpha(t_0,t_1) + \beta(t_1,t_2) + \alpha(t_2,t_3) + \cdots + \delta(t_{k-1},t_k), \quad (8)$$

where, $\delta(t_{j-1}, t_j)$ denotes $\alpha(t_{j-1}, t_j)$ if j is odd and $\beta(t_{j-1}, t_j)$ if j is even.

In order to calculate $\gamma(k, n)$, which is the least value of (1), we begin the calculation from $\gamma(1, t) = \alpha(1, t)$, for $t = 1, 2, \ldots, n$, and proceed by applying the formula

$$\gamma(m,t) = \min_{1 \le s \le t} \left[\gamma(m-1,s) + \delta(s,t)\right], \quad (9)$$

for $t = 1, 2, \ldots, n$, for every value of $m \in [2, k]$. We store also $\tau(m, t)$, namely the value of s that minimizes expression (9), for each value of m and t, and we always choose the smallest value of s.

At the end of the process, $m = k$ occurs and the sequence of optimal values $\{t_j : j = 1, 2, \ldots, k-1\}$ is obtained by the backward formula

$$t_{m-1} = \tau(m, t_m), \text{ for } m = k, k-1, \ldots, 2. \quad (10)$$

Accordingly, the components of an optimal fit are monotonic increasing on $[1, t_1]$ and on $[t_j, t_{j+1}]$ for even j in $[1, k-1]$ and monotonic decreasing on $[t_j, t_{j+1}]$ for odd j in $[1, k-1]$. This process requires $\mathcal{O}(kn^2)$ computer operations provided that all $\alpha(s, t)$ and $\beta(s, t)$ are available.

Certain extensions that improve the efficiency of this calculation are included in the software L1PMA. For instance, the numerical work is reduced at least by a factor of 4 if variable s in formula (9) is restricted at the indices of the local extrema of the data. Also, the software takes advantage of the fact that $\alpha(s, t)$ and $\beta(s, t)$ are independent of m, and makes full use of these numbers for all values of m, before incrementing t in (9). This is a major advancement of the calculation because we need not keep any extra storage and because $\alpha(s, t)$ and $\beta(s, t)$ are calculated only once on process.

The piecewise monotonic calculation depends on the efficiency of the algorithm that minimizes the objective function (5) subject to the constraints (6), which is a linear programming problem (see, Barrodale and Roberts [2]) that need not have a unique solution. Our method for calculating a best L_1 monotonic approximation is faster than applying general linear programming techniques because it takes into account the form of the constraints (6). Specifically, the calculation of a best monotonically increasing approximation to $\boldsymbol{\phi}$ seeks intervals where its components have different constant values. In the L_1 case these values are equal to the median of the corresponding data points, while in the L_2 case they are equal to their mean value. The intervals are formed by using the remarkable property that any constraints which are satisfied as equalities by a best L_1 approximation subject to a subset of the monotonicity constraints are also satisfied as equalities by a best L_1 approximation subject to all monotonicity constraints (6), which in essence is the method of van Eeden [15].

Further, the recommendation of Cullinan and Powell [5] that the specific value of the median should be chosen carefully in order that the final $\boldsymbol{y}$ satisfy the constraints (6) has been taken into account in the development of the best L_1 monotonic approximation algorithm that is included in [7]. This algorithm performs the calculation of a best L_1 monotonic increasing fit on $[t_{j-1}, t_j]$ together with all the numbers $\alpha(t_{j-1}, s) = \sum_{i=t_{j-1}}^{s} |y_i - \phi_i|, s = t_{j-1}, \ldots, t_j$ in $O((t_j - t_{j-1})^2)$ computer operations.

By taking account of these considerations, it is proved in [6] that a best L_1 approximation with at most k monotonic sections to the data is calculated in $\mathcal{O}(n^3 + kn^2)$ computer operations. This complexity reduces to $\mathcal{O}(n^2)$ when $k = 1$ or $k = 2$. The software package has been tested on a variety of data sets showing in practice quadratic performance with respect to n.

The method that gives a piecewise monotonic approximation may also be applied to the problem where inequalities (2) are replaced by the reversed ones, in which case the first section of the fit is decreasing. The latter problem may be treated computationally as the former one after an overall change of sign of $\boldsymbol{y}$. This is the case of the approximations that are presented in Section 3.2.

3 Peak Estimation of Some Spectra

In this section some examples demonstrate the performance of the L_1 method of Section 2 for peak estimation to real physical data. The data are the Raman, Infrared and NMR spectra of a mineral, an organic compound and, a human biological sample respectively, over a wide energy range, that were used by Demetriou and Perdikas [11] in their least squares

calculation. Our results are given in a way that the reader is instructively directed to distinguish the differences between these two calculations.

The results are presented in three subsections, one for each data set. The first and the third example are studied in the thesis of Perdikas [23] for the least squares case. The complexity of the underlying physical laws and the structural differences of the spectra make this a good test of the effectiveness of the best L_1 piecewise monotonic approximation method in peak estimation.

The data are far too many to be presented as raw numbers in these pages. However, one may easily capture the main features of each data set by looking at the corresponding figures. All the spectra contain important information contaminated with noise. Our choice of the data sets is due to the different levels of noise they present and the many isolated peaks that contain, which increase tremendously the number of all possible combinations of α's and β's in expression (8) if n and k are large. Indeed, as it is stated in the beginning of Section 2, if one tried to find the optimal integers $\{t_j : \ j = 1, 2, \ldots, k-1\}$, then the number of trials would be of magnitude n^{k-1}.

For every example, the software L1PMA is used to calculate the best L_1 piecewise monotonic approximation to the data sets and, the turning points of the best approximation. The data were fed to L1PMA without any preprocessing. To help readability, all the examples of this section are presented in the same format.

3.1 Raman Spectrum of Zircon

This subsection illustrates some features of the method of Section 2 by presenting an application to data from a Raman spectrum (for Raman spectroscopy see, for example, [22]). We downloaded the datafile named "zircon.txt", from the Raman spectra of minerals database, which is freely available on the website [14] of the University of Parma. The datafile contains $n = 1024$ pairs of data in a two-column format: The first column keeps the Raman shift (cm^{-1}) and the second column keeps the intensity (arbitrary units), providing the values $\{x_i : \ i = 1, 2, \ldots, n\}$ and $\{\phi_i : \ i = 1, 2, \ldots, n\}$, respectively for our calculations. The abscissae $\{x_i : \ i = 1, 2, \ldots, n\}$ are not needed to the recursive formula (9), but, of course, they are employed to show the positions of the peaks. We see in Fig. 1 that the data exhibit some distinct peaks, some peaks of lower intensity and small fluctuations.

We fed the data to L1PMA and the turning point positions obtained by the piecewise monotonic fits to the data for various values of k are given in Table 1. In the right hand side part of this table we give the positions of the turning points of each optimal fit for $k \in \{2, 4, 6, 8, 10, 12, 14, 16\}$ in correspondence with the column labeled "t_j" that is derived when $k = 16$. Thus, the times symbol in the cells of column "16" indicate the positions of the turning points when $k = 16$. Analogously, when $k = 6$ the turning points of the fit occur at the positions 188 (peak), 232 (trough), 265 (peak), 707 (trough) and 795 (peak) as indicated by the times signs in the column labeled "6". The sum of moduli of residuals and the maximum absolute residual of the fits associated with these columns is added to be able to evaluate the peaks of the resultant fit at a glance. For example, when $k = 6$ these quantities are equal to $\gamma(k = 6, n) = 1.19 \times 10^5$ and $D = 4.01 \times 10^3$.

We see in Table 1 that the sum of moduli of residuals decreased from 2.60×10^5 down to 1.69×10^4 as k increased from $k = 2$ to $k = 16$. Analogously, we see a gradual reduction in the values of the maximum absolute residual as k increased, which indicates that the best fit comes closer to the data.

As we also noted in [11], this is an important feature of the method that is not shared with smoothing techniques that involve splines or wavelets, for instance. Indeed, the latter methods suffer from the propagation effect when modeling a peak. In piecewise monotonic approximation, the presence of a peak does not cause at all any propagation effect. Therefore, there is no introduction of perturbations away from the peak. In other words, the piecewise monotonic approximation method avoids Gibb's ringing and is able to represent the data at a peak without becoming less accurate away from the peak. In this way, the piecewise monotonicity criterion not only is different from a low-pass filter, which is subject to the Gibbs effect (see, for example, Lanczos [19], Gasquet and Witomski [16]), but also very efficient in denoising signals and images (see, Lu [21] and Weaver [27]).

By comparing the columns of Table 1 with respect to the values of k, we notice that the extra turning points of the optimal approximation with $k+2$ monotonic sections occur between adjacent turning points of the optimal L_1 approximation with k monotonic sections. Although it is usual in practice that the turning points of an optimal fit with k monotonic sections are preserved by the optimal fit with $k + 2$ monotonic sections, one should be aware that this depends on the specific calculation and need not happen generally.

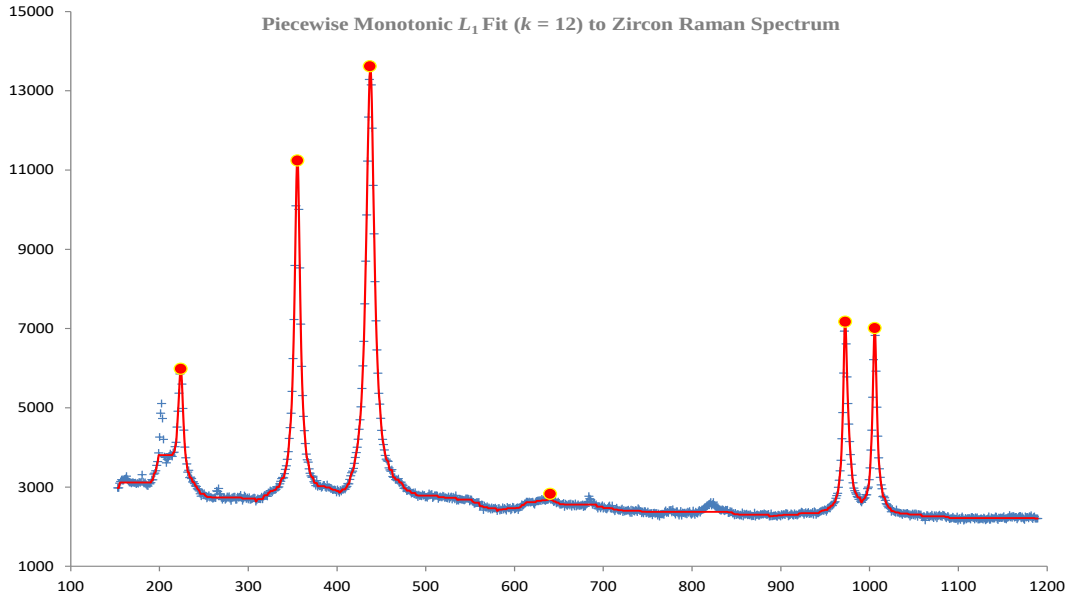

Figure 1: Detected peaks (circles) by a best L_1 fit with $k = 12$ monotonic sections to 1024 data points (plus signs) of the Zircon Raman spectrum. The solid line illustrates the best fit. The Raman shifts and the intensities are given in the x-axis and the y-axis, respectively.

Table 1: Left four columns: Turning points in the Zircon spectrum by a best L_1 fit with $k = 16$ monotonic sections. Right eight columns: The turning point positions of the optimal fit for $k \in \{2, 4, \ldots, 16\}$ are indicated by the times sign

j	t_j	x_{t_j}	ϕ_{t_j}	$k =$	2	4	6	8	10	12	14	16
0	1	153	2980		×	×	×	×	×	×	×	×
1	46	202	5110								×	×
2	51	208	3610								×	×
3	66	224	5950					×	×	×	×	×
4	144	309	2640					×	×	×	×	×
5	188	356	11200			×	×	×	×	×	×	×
6	232	403	2860			×	×	×	×	×	×	×
7	265	438	13600		×	×	×	×	×	×	×	×
8	402	580	2400							×	×	×
9	459	639	2740							×	×	×
10	582	763	2260									×
11	640	821	2620									×
12	707	887	2260				×	×	×	×	×	×
13	795	973	7140				×	×	×	×	×	×
14	814	991	2610						×	×	×	×
15	829	1010	6990						×	×	×	×
16	1024	1190	2210		×	×	×	×	×	×	×	×
				$\gamma(k, n) =$	2.60_5	1.82_5	1.19_5	5.97_4	3.18_4	2.56_4	2.09_4	1.69_4
				$D =$	8.07_3	4.77_3	4.01_3	4.01_3	1.30_3	1.30_3	2.47_2	2.27_2

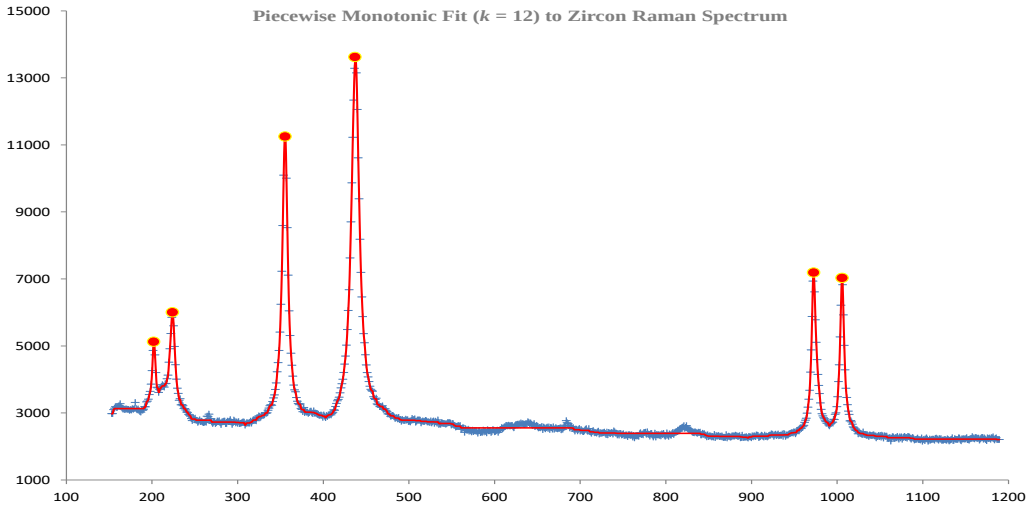

Figure 2: As in Fig. 1, but the detected peaks are found by the least squares fit with $k = 12$ of [11].

Table 2: As in Table 1, but by the least squares approximations of [11]

j	t_j	x_{t_j}	ϕ_{t_j}	$k =$	2	4	6	8	10	12	14	16
0	1	153	2980		×	×	×	×	×	×	×	×
1	46	202	5110							×	×	×
2	51	208	3610							×	×	×
3	66	224	5950					×	×	×	×	×
4	144	309	2640					×	×	×	×	×
5	188	356	11200			×	×	×	×	×	×	×
6	232	403	2860			×	×	×	×	×	×	×
7	265	438	13600		×	×	×	×	×	×	×	×
8	402	580	2400								×	×
9	459	639	2740								×	×
10	582	763	2260									×
11	643	824	2620									×
12	716	896	2250				×	×	×	×	×	×
13	795	973	7140				×	×	×	×	×	×
14	814	991	2610						×	×	×	×
15	829	1010	6990						×	×	×	×
16	1024	1190	2210		×	×	×	×	×	×	×	×

Demetriou and Perdikas [11] considered least squares piecewise monotonic approximations to these Raman data (see Demetriou and Powell [12], and Demetriou [8] for methods and software). For convenience we present in Table 2 results analogous to Table 1. A comparison of these tables shows that there are some differences between the turning point positions for certain values of k. The differences occur at the rows labeled $j = 1, 2, 8, 9$ when $k = 12$; $j = 11$ when $k = 16$; and, $j = 12$ when $k = 6, \ldots, 16$. In particular, the graphs of Figs. 1 and 2 illustrate the case when $k = 12$. Here, we see that the leftist two turning points of Fig. 2 do not appear in Fig. 1, and the eighth and ninth turning point of Fig. 1 do not appear in Fig. 2. However, the leftist two turning points of Fig. 2 enter the best L_1 fit when $k = 14$, as we see in Table 1. Further, the entries in the $j = 11, 12$ rows of Table 1 show a slight position shift of the corresponding turning points for each $k \in \{6, 8, \ldots, 16\}$ of Table 2.

3.2 Infrared Spectrum of Sulfonium Deuterated

In this subsection, we estimate peaks of the infrared spectrum of Sulfonium Deuterated (for Infrared spectroscopy see, for example, Larkin [20]). We downloaded the datafile named "SulfoniumDeuterated.jdx" from the PSLC Spectral Database of the website [13] of the Department of Chemistry, University of Wisconsin-Stevens Point. The datafile contains 2490 pairs of data in a two-column format, as described in Subsection 3.1. We capture the main features of these data by looking at Fig. 3. Indeed, we can see, for instance, very small deviations and some very distinguishable minima with sharp decreases.

We fed the data to L1PMA for $k = 2, 4, \ldots, 20$, while we required that the first monotonic section be decreasing. Table 3 presents results by analogy to Table 1, except that the t_j's, for even j, indicate lower turning points. We see in Table 3 that the sum of moduli of residuals decreased from 3.54×10^{10} down to 2.52×10^9 as k increased from $k = 2$ to $k = 20$, while the maximum absolute residual reduced from 3.80×10^8 down to 8.88×10^7. The results of the method for the infrared data are quite similar to those for the Raman data of Subsection 3.1. Hence, all the conclusions of Subsection 3.1 are valid for the infrared spectrum that we examine in this subsection.

In short, best L_1 piecewise monotonic approximation has revealed the most important turning points (minima and maxima), while it interpolated the data at these points. By increasing k, this approximation had the freedom to make the sum of the moduli of residuals smaller, while it maintained the most important turning points. It is remarkable that the method identified the sharp minima of the infrared spectrum, with no propagation effect when modelling them.

We consider the least squares piecewise monotonic approximation problem of [11] and for convenience we present in Table 4 results analogous to Table 3. A comparison of these tables shows that there are some differences between the turning point positions for certain values of k. Specifically, in Table 4 we see differences at the rows labeled $j = 8, 9, 18, 19$ when $k = 8$; $j = 6, 7, 15, 16$ when $k = 14$; and, $j = 1, 2, 3$ when $k = 20$. In particular, the graphs of Figs. 3 and 4 illustrate the case when $k = 14$. Further, the entries in the $j = 1, 2, 3$ rows of Table 4 for $k = 20$ indicate that the least squares approximation is rather unsatisfactory in the interval $[400, 425]$. Here, two turning points, at $x_3 = 403$ and $x_{18} = 425$, were inserted to combat a trend due possibly to data errors in the beginning of the range. As a consequence, this approximation did not detect the turning points at $x_{262} = 777$ and $x_{269} = 788$ of Table 3.

3.3 NMR Spectrum of Diiodothyronine

In this subsection, we estimate peaks of the human metabolome spectrum of diiodothyronine (for NMR spectroscopy see, for example, Gunther [17]). We downloaded the datafile named "diiodothyronine" from the website [4] of the Canadian Institute of Health Research. The diiodothyronine datafile contains 2167 pairs of data in a two-column format, as described in Subsection 3.1. We capture the main features of this data set by looking at Fig. 5. Indeed, we can see, for instance, tiny deviations and some very distinguishable peaks with quite sharp increases.

Table 5 presents some results by analogy to Table 1 for $k = 2, 4, \ldots, 16$. Here the sum of moduli of residuals decreased from 7.22×10^7 down to 5.95×10^6 as k increased from $k = 2$ to $k = 16$, while the maximum absolute residual reduced from 5.72×10^6 down to 9.88×10^4. The results of the method for the NMR data are similar to those for the Raman data of Subsection 3.1. Hence, all the conclusions of Subsection 3.1 are valid for the NMR spectrum that we examine in this subsection. However, it is worth repeating that despite the sharp increases of the peaks, the piecewise monotonic approximation method identified the peaks without any introduction of perturbations away from a peak.

We consider the least squares piecewise monotonic approximation problem of [11] and for convenience we present in Table 6 results analogous to Table 5. A comparison of these tables shows that there are slight differences between the turning point positions when $k = 4, 6, 8, 10$ at the intersection with the rows labeled $j = 10, 12, 14$. Further, Fig. 5 displays the resultant L_1 fit and the peaks when $k = 16$, which, in the scale of this page, is quite representative of the least squares analogue as well.

4 Conclusions

Peak estimation is an inherent problem in spectroscopy. In this paper, the best L_1 approximation method was used to estimate peaks of three sets of measurements of Raman, Infrared and NMR spectra. These data sets were chosen because they have essential differences and because they make it a difficult test of the effectiveness of the method.

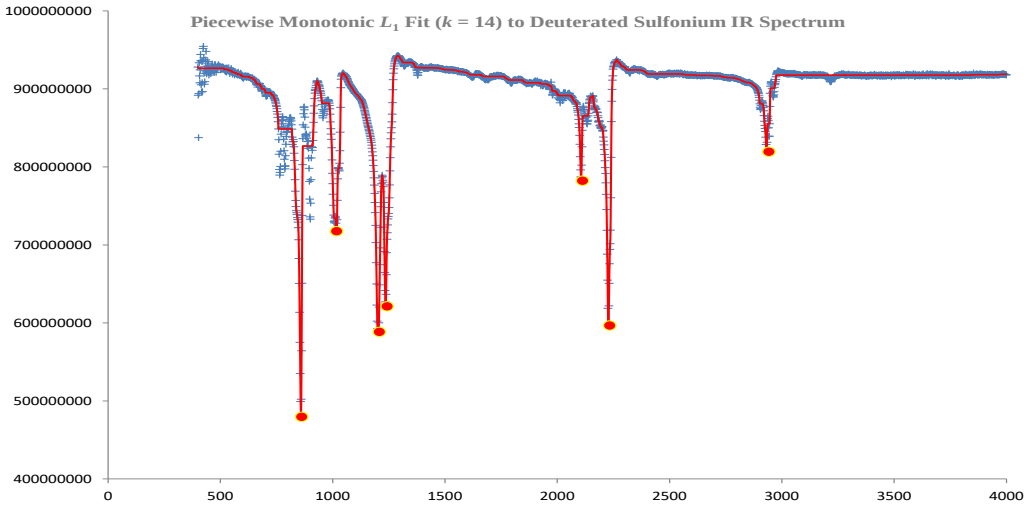

Figure 3: Detected minima (circles) by a best L_1 fit with $k = 14$ monotonic sections to 2490 data points (plus signs) of the Deuterated Sulfonium spectrum. The solid line illustrates the best fit. The intensities and positions of the turning points are presented in Table 3.

Table 3: Left four columns: Turning points in the Deuterated Sulfonium spectrum by a best L_1 fit with $k = 20$ monotonic sections. Right ten columns: The turning point positions of the optimal fit for $k \in \{2, 4, \ldots, 20\}$ are indicated by the times sign

j	t_j	x_{t_j}	ϕ_{t_j}	$k =$	2	4	6	8	10	12	14	16	18	20
0	1	400	927948672		×	×	×	×	×	×	×	×	×	×
1	253	764	789497984										×	×
2	262	777	864535616											×
3	269	788	797413056											×
4	285	811	863413760										×	×
5	318	858	482926432				×	×	×	×	×	×	×	×
6	328	873	876924160									×	×	×
7	347	900	732965248									×	×	×
8	368	931	910141824						×	×	×	×	×	×
9	428	1018	720472704						×	×	×	×	×	×
10	448	1047	920228736				×	×	×	×	×	×	×	×
11	556	1203	590654144		×	×	×	×	×	×	×	×	×	×
12	568	1220	789375680							×	×	×	×	×
13	579	1236	624402560							×	×	×	×	×
14	617	1291	942418048			×	×	×	×	×	×	×	×	×
15	1181	2107	786169536								×	×	×	×
16	1216	2157	891167616								×	×	×	×
17	1264	2227	598432640			×	×	×	×	×	×	×	×	×
18	1290	2264	937426688					×	×	×	×	×	×	×
19	1752	2932	818326272					×	×	×	×	×	×	×
20	2490	3999	917815168		×	×	×	×	×	×	×	×	×	×
				$\gamma(k,n) =$	3.54_{10}	2.21_{10}	1.36_{10}	9.68_{9}	6.08_{9}	4.99_{9}	4.11_{9}	3.28_{9}	2.86_{9}	2.52_{9}
				$D =$	3.80_{8}	3.80_{8}	1.54_{8}	1.54_{8}	9.85_{7}	9.37_{7}	9.37_{7}	8.88_{7}	8.88_{7}	8.88_{7}

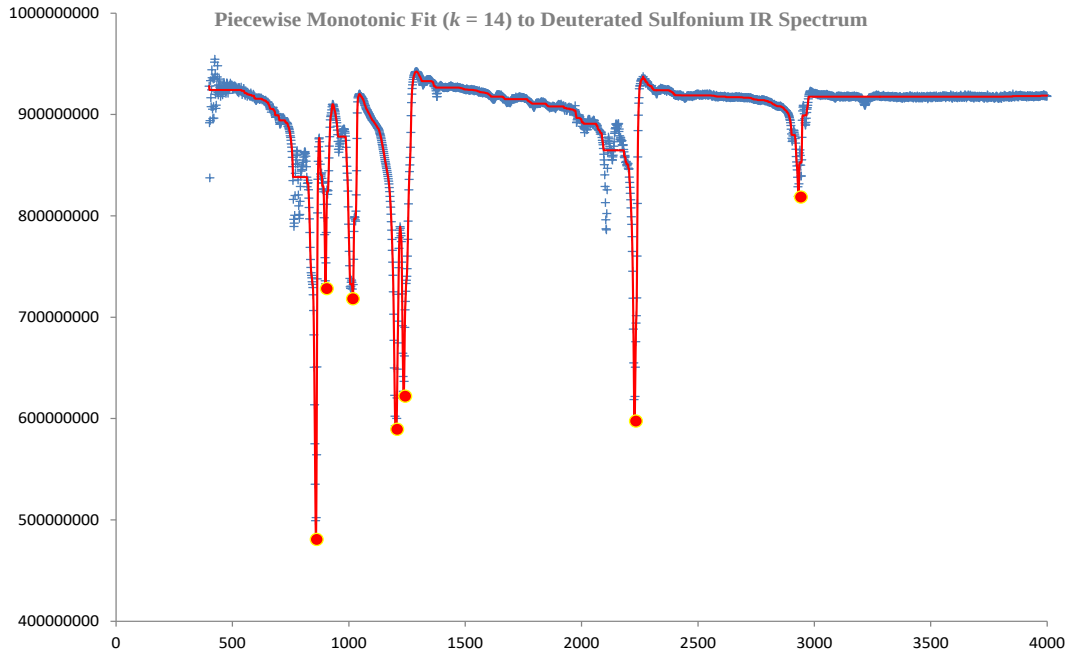

Figure 4: As in Fig. 3, but the detected minima are found by the least squares fit with $k = 14$ of [11]. The intensities and positions of the peaks are presented in Table 4.

Table 4: As in Table 3, but by the least squares approximations of [11]

j	t_j	x_{t_j}	ϕ_{t_j}	$k =$	2	4	6	8	10	12	14	16	18	20
0	1	400	927948672		×	×	×	×	×	×	×	×	×	×
1	3	403	837471680											×
2	18	425	954521536											×
3	253	764	789497984										×	×
4	285	811	863413760										×	×
5	318	858	482926432				×	×	×	×	×	×	×	×
6	328	873	876924160								×	×	×	×
7	347	900	732965248								×	×	×	×
8	368	931	910141824					×	×	×	×	×	×	×
9	428	1018	720472704					×	×	×	×	×	×	×
10	448	1047	920228736				×	×	×	×	×	×	×	×
11	556	1203	590654144		×	×	×	×	×	×	×	×	×	×
12	568	1220	789375680							×	×	×	×	×
13	579	1236	624402560							×	×	×	×	×
14	617	1291	942418048			×	×	×	×	×	×	×	×	×
15	1181	2107	786169536									×	×	×
16	1216	2157	891167616									×	×	×
17	1264	2227	598432640			×	×	×	×	×	×	×	×	×
18	1290	2264	937426688						×	×	×	×	×	×
19	1752	2932	818326272						×	×	×	×	×	×
20	2490	3999	917815168		×	×	×	×	×	×	×	×	×	×

We found that the best L_1 approximation method effectively captured the trends of the data and detected appropriate peaks as required by the values of k. We noticed that the extra turning points of the best L_1 approximation with $k+2$ monotonic sections occurred between adjacent turning points of the best approximation with k monotonic sections. However, this remark is of little help to the computation process, because it depends on the specific calculation and need not happen generally. It would have been quite interesting to investigate whether the separation properties for the turning points of least squares piecewise monotonic approximations that are presented by Demetriou [9] hold for the L_1 approximations as well.

We compared the results obtained by the best L_1 calculations to the analogous from least squares calculations. These results have shown many similarities as well as certain differences due to both properties of the used norms and nature of the spectra. Specifically, on the one hand, L1PMA calculates a best L_1 fit with at most k monotonic sections of the data in $O(n^3+kn^2)$ computer operations. However, the software package has been tested on a variety of data sets showing in practice quadratic performance with respect to n. The analogous least squares fit requires only $O(n^2 + kn\log n)$ computer operations, but in practice the results are far superior. On the other hand, we saw that there are some differences of the turning point positions for certain values of the number of monotonic sections, when considering the Raman and the Infrared spectra and, slight differences when considering the NMR spectrum.

As the numerical work for the L_1 case is about an order of magnitude higher than the work required by the least squares case, the effort of the L_1 task for estimating the turning points of the infrared spectrum of Section 3.2 was rewarded by the detection of an extra minimum when $k = 20$, which was not detected by the least squares calculation.

We restricted our work to the peak estimation problem of a spectrum and did not investigate particular fitting properties of a best approximation in the sense of the L_1 norm. We recall from Section 2 that the L_1 method employs a technique for calculating the median of subranges of data, while the least squares method calculates averages.

The examples of this paper have been discussed only with reference to the performance of the best L_1 piecewise monotonic approximation method, and not with a view to their interpretation in applications, which depends on the particular context. As a side note, the problem of peak location occurs in identifying stem cells, chemical substances and materials, and nebulae and galaxies from their spectra. The piecewise monotonic method is quite efficient for this purpose. So far the performance of the best L_1 piecewise monotonic approximation method for peak estimation of spectra was not known, while the examples were limited to peak estimation of only three types of spectra.

Our main contribution to the important problem of peak estimation of spectra is that we have provided a preliminary examination whose results draw attention to some interesting questions on the piecewise monotonic approximation that deserve further study and extensions to types of spectroscopy by application areas. Moreover, the given calculations suggest employing other norms as well in the piecewise monotonic approximation method that, depending on the particular spectra, will probably give appropriate peak estimations. Indeed, the analyst would be helped by comparing results of piecewise monotonic approximation when various norms are used.

Further, one could apply the piecewise monotonic approximation method presented here to a variety of situations where the analyst knows some properties of the data being collected and studied, as for example in the biological signals of Augustyniak [1], or the periodic and quasi-periodic signals of Scholkmann, Boss and Wolf [25].

Acknowledgements: The authors are grateful to three referees for useful comments that improved the presentation of the paper.

References:

[1] P. Augustyniak, Time-Frequency Integration of Variable-Bandwidth Signals and Supplementary Data Packets, *International Journal of Biology and Biomedical Engineering*, 2018, 12, pp. 114–123.

[2] I. Barrodale and F. D. K. Roberts, An efficient algorithm for discrete ℓ_1 linear approximation with linear constraints, *SIAM J. Numer. Anal.*, 1978, 15, pp. 603–611.

[3] C. de Boor, *A Practical Guide to Splines, Revised Edition*, NY: Springer-Verlag, Applied Mathematical Sciences, vol. 27, 2001.

Table 5: Left four columns: Turning points in the Diiodothyronine spectrum by a best L_1 fit with $k = 16$ monotonic sections. Right eight columns: The turning point positions of the optimal fit for $k \in \{2, 4, \ldots, 16\}$ are indicated by the times sign

j	t_j	x_{t_j}	ϕ_{t_j}	$k =$	2	4	6	8	10	12	14	16
0	1	50	458		×	×	×	×	×	×	×	×
1	899	288	91294									×
2	933	290	248									×
3	1076	325	137208								×	×
4	1253	343	196								×	×
5	1297	353	379883							×	×	×
6	1453	366	196							×	×	×
7	1569	382	2099943				×	×	×	×	×	×
8	1743	417	196				×	×	×	×	×	×
9	1848	467	435337						×	×	×	×
10	1891	470	248						×	×	×	×
11	1910	480	7030589		×	×	×	×	×	×	×	×
12	1990	485	241			×	×	×	×	×	×	×
13	2050	509	1015734					×	×	×	×	×
14	2089	516	196					×	×	×	×	×
15	2107	526	5725926			×	×	×	×	×	×	×
16	2167	550	275		×	×	×	×	×	×	×	×
				$\gamma(k,n) =$	7.22_7	3.52_7	1.94_7	1.41_7	1.09_7	7.79_6	6.65_6	5.95_6
				$D =$	5.72_6	2.10_6	1.01_6	4.31_5	3.78_5	1.35_5	9.88_4	9.88_4

Table 6: As in Table 5, but by the least squares approximations of [11] [a]

j	t_j	x_{t_j}	ϕ_{t_j}	$k =$	2	4	6	8	10	12	14	16
0	1	50	458		×	×	×	×	×	×	×	×
1	899	288	91294									×
2	938	292	196									×
3	1076	325	137208								×	×
4	1253	343	196								×	×
5	1297	353	379883							×	×	×
6	1453	366	196							×	×	×
7	1569	382	2099943				×	×	×	×	×	×
8	1743	417	196				×	×	×	×	×	×
9	1848	467	435337						×	×	×	×
10	1891	470	248						□	×	×	×
11	1910	480	7030589		×	×	×	×	×	×	×	×
12	1990	485	241			○	○	×	×	×	×	×
13	2050	509	1015734					×	×	×	×	×
14	2089	516	196					◇	◇	×	×	×
15	2107	526	5725926			×	×	×	×	×	×	×
16	2167	550	275		×	×	×	×	×	×	×	×

[a] $\times$ = the number in column labeled "t_j", $\square = 1889$, $\circ = 2000$, $\diamond = 2087$

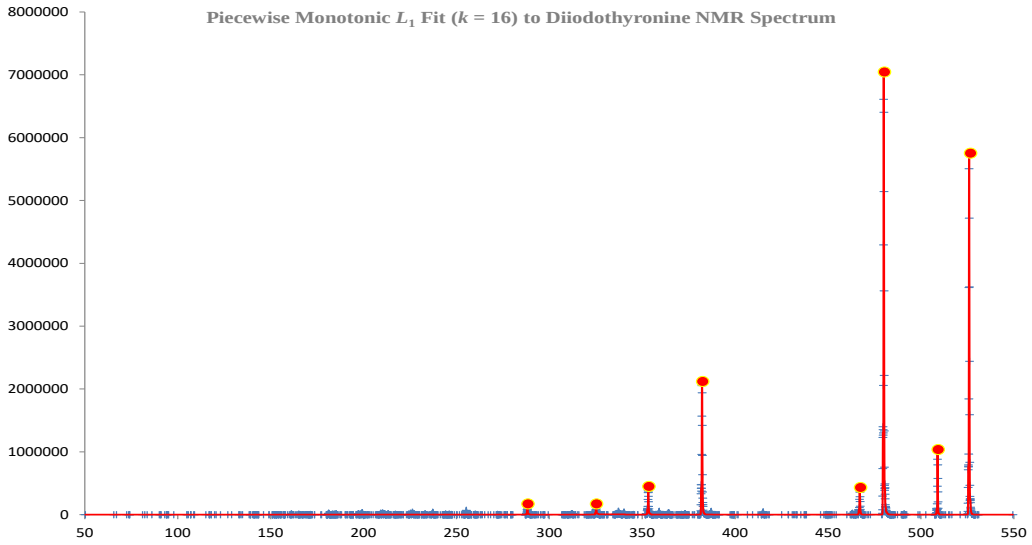

Figure 5: Detected peaks (circles) by a best L_1 fit with $k = 16$ to 2167 data points (plus signs) of the Diiodothyronine NMR spectrum. The solid line illustrates the best fit. The intensities and positions of the peaks are presented in Table 5

[4] Canada Foundation for Innovation and The Metabolomics Innovation Centre (TMIC), Canadian Institutes of Health Research. Available online: http//www.hmdb.ca/metabolites, Database, Human Metabolome Database, Diiodothyronine.txt, accessed 10 January 2019.

[5] M. P. Cullinan and M. J. D. Powell, Data smoothing by divided differences. In: *Numerical Analysis Proc. Dundee 1981* (ed. G. A. Watson), LNIM 912, Berlin: Springer-Verlag, 26–37, 1982.

[6] I. C. Demetriou, Best L_1 piecewise monotonic data modelling, *Int. Trans. Opl Res.*, 1994, 1, 1, pp. 85–94.

[7] I. C. Demetriou, L1PMA: A Fortran 77 package for best L_1 piecewsie monotonic data smoothing, *Computer Physics Communications*, 2003, 151, 1, pp. 315–338.

[8] I. C. Demetriou, Algorithm 863: L2WPMA, a Fortran 77 package for weighted least-squares piecewise monotonic data approximation, *ACM Trans. Math. Softw.*, 2007, 33, 1, pp. 1–19.

[9] I. C. Demetriou, Separation theorems for the extrema of best piecewise monotonic approximations to successive data, *Optimization Methods and Software*, 2020, 35, 3, pp. 439–459. DOI: 10.1080/10556788.2019.1613653

[10] I. C. Demetriou, A characterization theorem for the best L1 piecewise monotonic data approximation problem. In *Contributions in Mathematics and Engineering. In Honor of Constantin Carathéodory* (editors: Panos M. Pardalos, Themistocles M. Rassias. Forward by R. Tyrrell Rockafellar), Springer International Publishing, Switzerland, 2016, pp. 117–126.

[11] I. C. Demetriou and I. N. Perdikas, The effectiveness of the piecewise monotonic approximation method for the peak estimation of noisy univariate spectra. In *Proceedings of the 2019 International Conference on Control, Artificial and Optimization (ICCAIRO 2019)*, December 8-10, 2019, Athens, pp. 69–77, 2020 (978-1-7281-3572-4/1 ©2019 IEEE. DOI 10.1109/ ICCAIRO47923.2019.00020).

[12] I. C. Demetriou and M. J. D. Powell, Least squares smoothing of univariate data to achieve piecewise monotonicity, *IMA J. of Numerical Analysis*, 1991, 11, pp. 411–432.

[13] Department of Chemistry, University of Wisconsin-Stevens Point. Available online: https://pslc.uwsp.edu, Database, PSLC Spectral Database, SulfoniumDeuterated.jdx, accessed 15 November 2019.

[14] Department of Physics, University of Parma. Available online: http//www.fis.unipr.it/phevix/ramandb.php, Database, Laboratory of Photoinduced Effects Vibrational and X-RAYS Spectro-

scopies, Minerals, Zircon1.txt, accessed 12 December 2018.

[15] C. van Eeden, Maximum likelihood estimation of ordered probabilities, *Indag. Math.*, 1956, 18, pp. 444–455.

[16] C. Gasquet and P. Witomski, *Fourier Analysis and Applications. Filtering, Numerical Computation, Wavelets*, Translated by R. Ryan, Springer-Verlag, NY 1999.

[17] H. Gunther, *NMR Spectroscopy: Basic Principles, Concepts and Applications in Chemistry*, 3rd ed., J. Wiley and Sons Chichester, U. K. 2013

[18] M. Holschneider, *Wavelets. An Analysis Tool*, Clarendon Press, Oxford 1997.

[19] C. Lanczos, *Applied Analysis*, Pitman and Sons, U. K. 1957.

[20] P. J. Larkin, *IR and Raman Spectroscopy, Principles and Spectral Interpretation*, Elsevier, U. K. 2011.

[21] J. Lu, Signal restoration with controlled piecewise monotonicity constraint. In *Proceedings of the IEEE International Conference on Acoustics, Speech and Signal Processing*, 12-15 May 1998, Seattle WA, 3, pp. 1621–1624, 1998.

[22] R. L. McCreery, *Raman Spectroscopy for Chemical Analysis*, J. Wiley and Sons, Chichester, U. K. 2000.

[23] I. N. Perdikas, *Numerical Evidence of the Lagrange Multipliers in Piecewise Monotonic Data Approximation*, MSc Thesis, Department of Economics, National and Kapodistrian University of Athens, 65 pp., 2019.

[24] M. J. D. Powell, *Approximation Theory and Methods*, Cambridge University Press, Cambridge, U.K. 1981.

[25] F. Scholkmann, J. Boss and M. Wolf, An Efficient Algorithm for Automatic Peak Detection in Noisy Periodic and Quasi-Periodic Signals, *Algorithms*, 2012, 5, pp. 588–603.

[26] R. J. Urban, W. S. Evans, A. D. Rogol, D. L. Kaiser, M. L. Johnson and J. D. Velduhuis, Contemporary Aspects of Discrete Peak-Detection Algorithms. The Paradigm of Luteinizing Hormone Pulse in Men, *Endocrine Reviews*, 1988, 9, 1, pp. 3–37.

[27] J. B. Weaver, Applications of Monotonic Noise Reduction Algorithms in fMRI, Phase Estimation, and Contrast Enhancement, *International Journal on Innovation, Science and Technology*, 1999, 10, pp. 177–185.